Translational Oncology 14 (2021) 100953

Contents lists available at ScienceDirect

Translational Oncology

journal homepage: www.elsevier.com/locate/tranon

Cell by cell immuno- and cancer marker profiling of non-small cell lung cancer tissue: Checkpoint marker expression on CD103+, CD4+ T-cells predicts circulating tumor cells

Xiaoyang Wang[a], Maria Jaimes[b], Huimin Gu[b], Keith Shults[a], Santosh Putta[c], Vishal Sharma[d], Will Chow[d], Priya Gogoi[d], Kalyan Handique[d], Bruce K Patterson[a,*]

[a] IncellDx Inc, 1541 Industrial Road, San Carlos, CA, United States
[b] Cytek Biosciences Inc, Fremont, CA, United States
[c] Qognit Inc, San Carlos, CA, United States
[d] Celsee Inc, Plymouth MI, United States

ARTICLE INFO

Key words:
Circulating tumor cell
CTLA-4
LAG3
CCR5
Cancer marker
High parameter flow cytometry
Non-small cell lung cancer
Aneuploidy
Tumor infiltrating lymphocyte
Tumor microenvironment

ABSTRACT

Non-small cell lung cancer (NSCLC) has a poor prognosis. Targeted therapy and immunotherapy in recent years has significantly improved NSCLC patient outcome. In this study, we employed cell-by-cell immune and cancer marker profiling of the primary tumor cells to investigate possible signatures that might predict the presence or absence of circulating tumor cells (CTCs). We performed a comprehensive study on 10 NSCLC patient tissue samples with paired blood samples. The solid tissue biopsy samples were dissociated into single cells by non-enzymatic tissue homogenization and stained with a total 25 immune, cancer markers and DNA content dye and analyzed with high-parameter flow cytometry. CTCs were isolated and analyzed from the paired peripheral blood. We investigated a total of 74 biomarkers for their correlation with CTC number. Strong correlations were observed between CTC number and the frequency of immune checkpoint marker expressing lymphocytes (CTLA-4, LAG3, TIM3, PD-1), within the $CD103^{+}CD4^{+}$ T lymphocyte subset. CTC number is also correlated with the frequency of PD-L1 expressing cancer cells and cancer cell DNA content. In contrast, CTC number inversely correlated to the frequency of $CD44^{+}$E-cadherin^{-} cancer cells. Unsupervised clustering analysis based on the biomarker analysis separated the CTC negative patients from the CTC positive patients. Profiling multiple immune and cancer markers on cancer samples with multi-parametric flow cytometry allowed us to obtain protein expression information at the single cell level. Clustering analysis of the proteomic data revealed a signature driven by checkpoint marker expression on $CD103^{+}CD4^{+}$ T cells that could potentially be predictive of CTCs and targets of therapy.

Introduction

Lung cancer is the number one cause of cancer death in both men and women in the U.S. and worldwide. NSCLC is the most common type, accounting for about 80–85% of the lung cancers. Most NSCLC has a poor prognosis since the patients are normally at the advanced stage of the cancer development at diagnosis.

The traditional treatments with surgical removal, radiation therapy, and chemotherapy have made slow progress and provided limited improvement in the 5-year survival rate [1–2]. On the other hand, the recent advancement in targeted therapy and immunotherapy has demonstrated the restoration of immunity against the tumor cells and control of tumor spread [3].

Immunotherapy has emerged as a new treatment option for lung cancer although only 20% of NSCLC have long-lasting response [4]. Immunotherapy, more specifically checkpoint inhibitors, act to boost the body's natural defenses to fight the cancer by way of the PD-1/PD-L1 pathway. Antibodies against PD-1, Nivolumab (Opdivo) and pembrolizumab (Keytruda), against PD-L1, Atezolizumab (Tecentriq) have been successfully developed to block the PD-1 and PD-L1 ligation and have been approved by the FDA for NSCLC treatment [5].

Some of these other checkpoint markers, such as CTLA-4, LAG-3 and TIM-3, are also emerging targets for NSCLC treatment. Antibod-

Abbreviations: PD-1, programmed death-1; PD-L1, programmed death-ligand 1; TIM-3, mucin domain-3-containing molecule-3; LAG-3, lymphocyte-activation gene-3; CTLA-4, cytotoxic T-lymphocyte antigen-4; CCR5, CC chemokine receptor 5; EGFR, epidermal growth factor receptor; ALK, anaplastic lymphoma kinase; TIL, tumor infiltrating lymphocyte; TME, tumor microenvironment.

* Corresponding author.
E-mail address: brucep@incelldx.com (B.K. Patterson).

https://doi.org/10.1016/j.tranon.2020.100953
Received 15 September 2020; Received in revised form 2 November 2020; Accepted 9 November 2020

Table 1
Clinical characteristics of study patients.

Sample ID	Histology	Gender	Age	Stage	Metastasis
1	SCC	M	67	Stage III	Y
2	AC	M	76	Stage II	Y
3	AC	F	68	Stage II	N
4	AC	F	81	Stage III	N
5	SCC	M	63	Stage II	N
6	AC	M	71	Stage III	Y
7	AS	F	77	Stage IV	Y
8	SCC	M	83	Stage III	Y
9	SCC	F	74	Stage III	Y
10	AC	M	61	Stage III	Y

SCC-squamous cell carcinoma, AC-adenocarcinoma, AS-adenosquamous carcinoma.

ies against CTLA-4 have been approved for treating some cancer types while the co-inhibitory effect of CTLA-4 and PD-1 blockade may make it a good candidate in combination with anti-PD-1 to treat NSCLC [6]. Anti-LAG-3 is in clinical trials to treat NSCLC [7] and evidence also suggests that TIM-3 will be a good target for immunotherapy for several cancer types including NSCLC [8].

Nearly 40% of newly diagnosed lung cancer patients have tumors that have already metastasized. During cancer development, tumor epithelial cells transit into mesenchymal cells [EMT] followed by entrance into the blood circulation to become circulating tumor cells [CTCs]. CTCs are considered to be the precursors of tumor dissemination and metastasis and the CTC number is directly associated with cancer metastasis and poor prognosis [9].

As such, CTCs have also been used extensively as early markers of response to checkpoint inhibitors [9].

Since the checkpoint inhibitors only produce long term survival in 20% of individuals, other biomarkers to predict response to checkpoint inhibitors would be desirable [4].Here, we present a pilot study to ask whether immune cell subsets can predict the presence of CTC in NSCLC and further aid in patient management.

In this study, we applied advanced flow cytometry technology, studying 25 cancer and immune markers with DNA content in the same samples. Combining cancer and immune markers with DNA content is unique as DNA content is an idependent factor that is associated with poor prognosis and can be directly measured by abnormal DNA quantity (aneuploidy) [10, 11]. Out of the 26 unique cell marker studied, we investigated the expression of a total of 72 biomarkers that result from using combinations of cellular markers in our algorithm to predict CTCs.

Material and methods

Samples

Fresh tissues were obtained from 10 NSCLC cases by Folio Biosciences [Powell, OH] with paired peripheral blood sample following informed consent. Date of collection, age, sex, ethnicity, diagnosis, primary tumor size and American Joint Committee on Cancer [AJCC] classification were recorded (Table 1). Samples were collected at the time of diagnosis. Tissues were excised and then stored in Roswell Park Memorial Institute [RPMI] 1640 medium at 2–8°C prior to overnight shipment to IncellDx Inc. [San Carlos, CA] on cold packs. The blood samples from the same patients were shipped to and processed at Celsee Inc. [Ann Arbor, MI]

Tissue dissociation using incellPREP

Tissue dissociation into single cell suspension were performed as previously described [12, 13]. Briefly, tumor tissue was first made into 4-mm punches, and placed in 2-mL Eppendorf tubes containing 800 μL Dulbecco's phosphate-buffered saline [DPBS]. *Incell*PREP tissue homogenizers [IncellDx, Inc.] were inserted into each tube and tissue was homogenized until cloudy (5–10 min). After tissue homogenization, the supernatants were collected and centrifuged. Following centrifugation, the cell pellet was resuspended in *incell*MAX [IncellDx, Inc] reagent at a concentration of 1×10^6 cells/mL and incubated at room temperature for 1 hour prior to staining.

Immune and cancer marker panel staining of single cell suspensions

The cancer markers or immune markers were used for staining all samples. The staining was performed in DPBS + 2 % bovine serum albumin (BSA) buffer and incubated for 30 min at room temperature in the dark. Then the samples were washed twice in 1 mL of DPBS + 2 % BSA. After the final wash, the cell pellets were reconstituted in 300 μL of DPBS for the immune marker panel before being acquired on a flow cytometer. For cancer marker tubes, an additional step of staining with 200 μL of cell cycle dye (IncellDx, Inc) at 1 μg/mL concentration in DPBS was performed. 100,000 to 500,000 cells were stained for each tube. The cancer and immune markers used for staining are listed in the Supplemental Table 1.

Flow cytometry

The cells stained with the immune marker panel were analyzed on a Cytek Aurora™ cytometer equipped with three lasers (Cytek Biosciences Inc). The cells stained with the cancer marker panels were analyzed on a 3-laser CytoFLEX™ cytometer (Beckman Coulter). DNA index was calculated as cell cycle dye staining MFI (median fluorescent intensity) of cancer cells divided by diploid cell (lymphocytes in this study) MFI.

CTC isolation and enumeration

Patient peripheral blood samples were received in a Streck cfDNA BCT® (Streck Inc.) and kept at ambient temperature. 4mL of the blood samples was prefixed using incellMAX® reagent (IncellDx, Inc) for 10 min (Supplemental Fig. 1). Following pre-fixation, the sample was then diluted three-fold with 1x HBSS. Each sample was then processed utilizing the Celsee CellSelect™ Preparation chip, Genesis automated platform, and enumeration protocol. Upon completion, the chips were scanned on the Celsee Analyzer™ where a final report was generated. Each individual cell was assessed for detection of CD45, CK, PD-L1 and DNA content (cell cycle dye) [14, 15]. Cells were captured in the 50,000 microwells and stained for CD45, CK, PD-L1, and cell cycle as a cocktail

Visualization of single cell lymphocyte data

In order to visualize the high dimension single cell data, Uniform Manifold Approximation and Projection (UMAP) [16] was applied to the data using Ryvett [www.qognit.com/products] software package from Qognit Inc. UMAP is a dimensionality reduction technique, similar to t-SNE [17], which aims to preserve the relative local distances between points [cells] from the original high-dimensional space in the lower [projection] dimensional space. UMAP was applied to enable the visualization of high-dimensional data to discovery patterns. Unlike techniques like principal component analysis [PCA] which focus on preserving the global distance structure, UMAP focusses on preserving the local distances [neighborhood] of each point more accurately in the projection space.

Results

CTC isolation and analysis

To determine the analytical performance of our CTC method prior to analysis of patient samples, we performed PD-L1$^+$ tumor cell spiking ex-

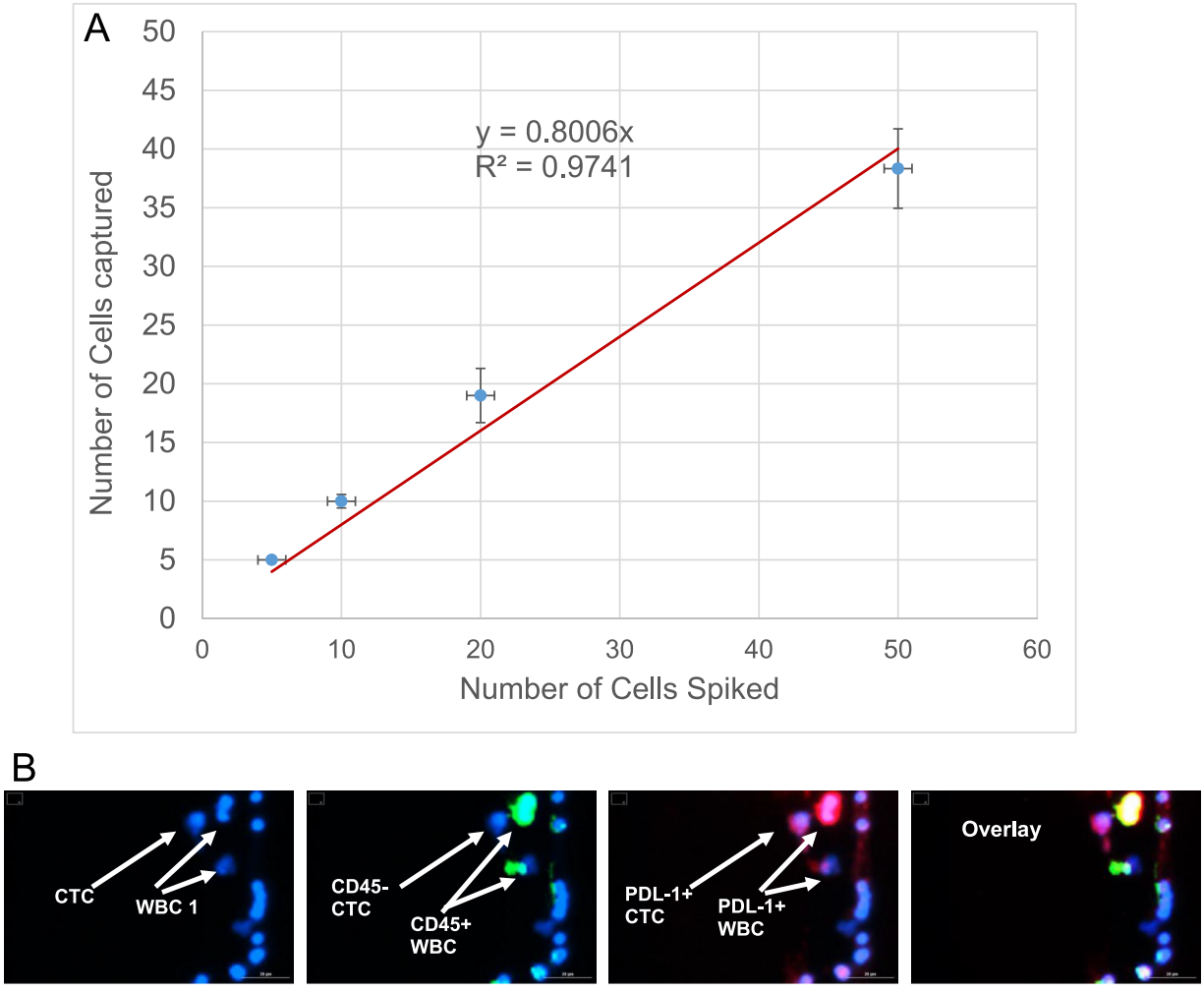

Fig. 1. CTC enumeration and analysis. (A). Spiking analysis for CTC recovery. NCI-441 cells [PD-L1 positive lung cancer cell line] were spiked into normal blood sample. Five cells can be detected in 4 mL normal blood with greater than 80% recovery. (B). Representative images showing CD45 negative, CK+, and PD-L1 positive cells captured in the CelSelect microfluidic chip microwells as determined by DAPI staining.

periments in normal blood to determine the lower limits of reproducible detection and the linearity across target cell concentrations. As shown in Fig. 1(A), we were able to reproducibly detect 5 PD-L1^{+} tumor cells (OncoTect iO control cells, IncellDx, Inc) spiked in 4 mL of whole blood with a linear range from 5 PD-L1 target cells to 50 target cells per 4 mL of whole blood as captured on the CelSelect chip in the Genesis Analyzer. This approach has been previously shown to be more sensitive than the established CellSearch method [15]. Seven of the 10 samples had detectable CTC counts ranging from 81 CTCs to 0 per 4 mL of whole blood. A representative image from Patient 1 is shown in Fig. 1(B) and demonstrates the optimized staining of the individual markers (CD45, cytokeratin, PD-L1, and DAPI) as well as the overlay of the images. Cells that are CD45-, CK+ are considered epithelial and enumerated.

Predictive markers of CTCs: cancer marker expression

To determine the expression profile of tumor cells in NSCLC samples that might contribute to tumor growth and dissemination, we generated single cell suspensions from the tumor tissue as described in Materials and Methods and using a workflow described by the College of American Pathologist [CAP] for lymphoma samples [18]. We gated single nucleated cells using light scatter and cell cycle dye staining [see Fig. 2] and we also used cell cycle dye staining also to separate tumor cells with high DNA content [aneuploid cells] from cells with normal DNA content [diploid cells]. The “Aneuploid” gate includes cells with higher DNA content, a consequence of either chromosomal level mutation resulting in increased chromosome number [reflecting tumor mutation burden, TMB] or due to increased cell proliferation or both. Simultaneous DNA staining also provided the MFI values for DNA index calculations. Representative plots are shown in Fig. 2 and the correlation with CTCs is summarized in Table 2. The presence of CD44+, Ecad- cells negatively correlated with CTCs and PD-L1 expression on aneuploid tumor cells positively correlated with CTCs. Both were statistically significant. Table 3.

Among the other cancer markers studied, EGFR expression was observed in all the cancer samples investigated and was observed in both diploid and aneuploid cells. ALK fusion was observed in one cancer sample, which is consistent with the previous observation that 3–7% of the NSCSC samples harbor the ALK fusion. Interestingly, the ALK mutated cells also highly expressed EGFR and had higher DNA content [Fig. 2]. As expected in NSCLC, the majority of the cancer cells are epithelial cells (CK^{+}) admixed with a smaller portion of cells of mesenchymal/stromal origin (vimentin$^{+)}$. We found some cells that were pan CK and vimentin double positive suggesting a possible link to the epithelial/mesenchymal cell transition [EMT] [8]. Of note, the true mesenchymal cells were diploid yet the double positive EMT cells were aneuploid when the primary cancer cells were aneuploidy consistent with the tumor phenotype.

In addition to tumor, mesenchymal, and immune cells, we identified cells in all samples expressing the CD44 positive, E-cadherin (E-cad) negative phenotype. CD44 is a cancer stem cell marker and E-cad plays

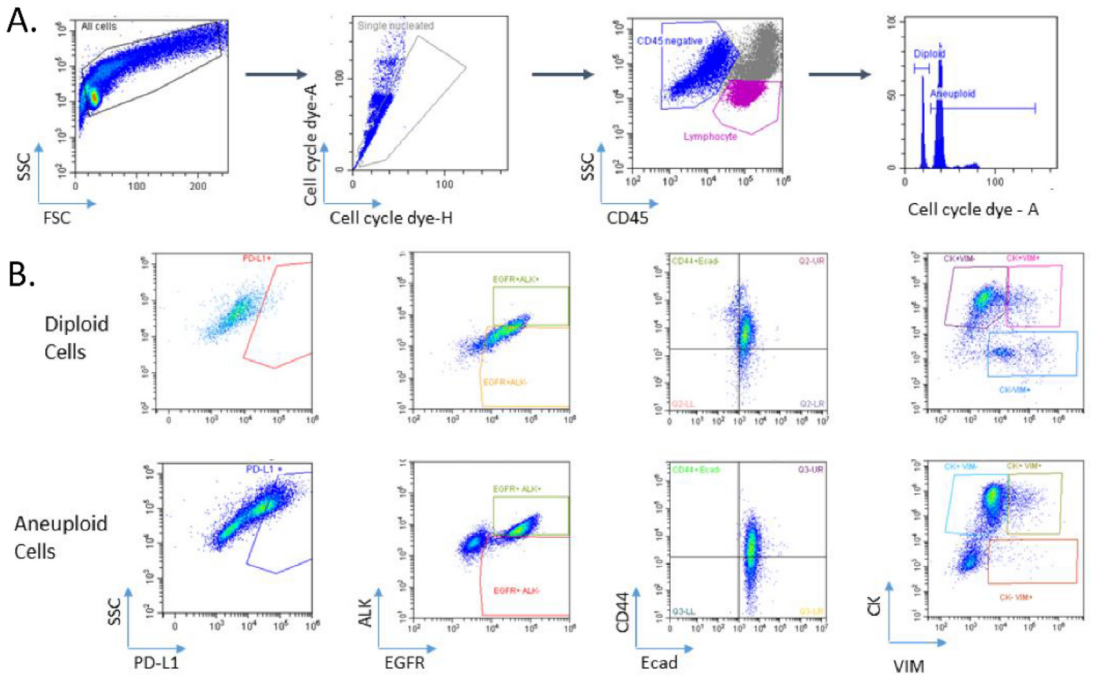

Fig. 2. Flow analysis of cancer marker expression.
(A). Single nucleated cells were gated using forward, side scatters and cell cycle dye staining. CD45 negative cancer cells were separated into diploid and aneuploidy cells based on cell cycle dye DNA content staining.
(B). Cancer markers were interrogated on diploid and aneuploidy cancer cells separately. Data presented is from Sample 1

Table 2
Spearman R statistical data analysis results for cancer cells with P values. The percentages of cells used for the statistical analysis were taken as a fraction of total $CD45^-$ cancer tissue cells except All Tumor cells is taken as a fracture of all cells from the tumor tissue. Data with a Spearman R absolute value greater than 0.5 are highlighted in yellow. R: Spearman R.

	Marker	Parent Population	R	P
Tumor	DNA Index	Tumor	0.52	0.13
	cCaspase 3+	Tumor	-0.22	0.54
	pH2AX+	Tumor	0.14	0.70
	Tumor Cells	All cells	0.07	0.85
	CD44+Ecad-	Tumor	-0.70	0.02
	CK+VIM+	Tumor	-0.30	0.39
	CK-low VIM+	Tumor	-0.09	0.80
	EGFR+	Tumor	0.20	0.58
	PD-L1	Tumor	0.55	0.10
Aneuploid Tumor	Tumor Cells	Tumor	0.24	0.51
	CD44+Ecad-	Tumor	-0.03	0.93
	CK+VIM+	Tumor	0.04	0.91
	CK-low VIM+	Tumor	-0.14	0.70
	EGFR+	Tumor	0.49	0.15
	PD-L1	Tumor	0.57	0.05
Diploid Tumor	Tumor Cells	Tumor	-0.24	0.51
	CD44+Ecad-	Tumor	-0.69	0.03
	CK+VIM+	Tumor	-0.37	0.29
	CK-low VIM+	Tumor	0.02	0.96
	EGFR+	Tumor	-0.22	0.54
	PD-L1	Tumor	0.08	0.89

an important role in epithelial cell adhesion and the loss of its function is considered to be a major contributor to epithelial mesenchymal transition (EMT) [8]. We found that the distribution of $CD44^+$E-cad^- cells were present at various levels in different tumors.

Using this cancer marker panel (Supplemental Table 2), lymphocytes did not exhibit DNA damage [histone pH2A.x (ser 139) staining negative], however, a significant percentage of the lymphocytes were undergoing apoptosis as shown by the cleaved caspase 3 staining. Fewer cancer cells were apoptotic compared to lymphocytes yet the cancer cells exhibited higher levels of DNA damage compared to lymphocytes, as evidenced by positive pH2A.x staining. DNA damage and apoptosis, however, did not correlate with the presence or absence of CTCs in peripheral blood.

Immune check point marker expression in the tumor microenvironment

To determine the immune profile in the tumor microenvironment and to investigate the possible role in loss of immune control and CTCs, we used the same single cell suspension used for the cancer marker expression to interrogate a total of 19 markers simultaneously on every cell in a single tube. The single cell suspension samples were stained with markers for gating to separate cancer immune cell subsets and immune check point markers, along with HLA-DR, an immune activation marker, and CD103, a marker indicating the engagement of immune cells with cancer cells [19, 20].

The cells were separated into immune cell subsets by gating markers, immune check point markers, and immune function markers (Fig. 3(A)). $CD4^+$ and $CD8^+$ T cells were variable across samples while a low percentage of NK cells was observed in the ten NSCLC samples. PD-1, CTLA-4, LAG-3, TIM-3, HLA-DR, and CD103 showed differential expression on these cell subpopulations as presented in Supplemental Table 3.

In order to visualize the high dimension single cell data, we applied UMAP on the 19-color panel data as described in Materials and Methods. The representative data is shown in Fig. 3(B). The UMAP separated $CD4^+$, $CD8^+$ T cells, NK cells, and B cells in very distinctive populations. In addition, in some samples $CD4^+$ and $CD8^+$ cells were further divided into subpopulations. We interrogated each marker on these cells. It appeared that CD103 is a driver for the segregation of these $CD4^+$ and $CD8^+$ cells into subpopulations. More importantly, overlaying the UMAP plots with positivity for checkpoints suggested that the positivity, when present, was often concentrated among the $CD103^+$ cells.

Table 3
Spearman R statistical data analysis results for TILs with P values. The percentages of cells used in the statistical analysis were either taken as a fraction of total TILs [lymph], or as a fraction of a TIL subpopulation [CD4$^+$ T, CD8$^+$ T, or NK]. Data with a Spearman R greater than 0.5 are highlighted in yellow. The irrelevant cells are shaded in grey. R: Spearman R.

		Marker	Parent Population							
			Lymph		CD4+ T		CD8+ T		NK	
			R	P	R	P	R	P	R	P
Marker Detection Population	Lymph	PD1+	0.756	0.011						
		TIM3+	0.634	0.049						
		CTLA4+	0.530	0.115						
		LAG3+	0.451	0.191						
		CD103+HLADR	0.677	0.032						
	CD4+ T	PD1+	0.787	0.007	0.689	0.028				
		TIM3+	0.756	0.011	0.689	0.028				
		CTLA4+	0.384	0.273	0.384	0.273				
		LAG3+	0.732	0.016	0.518	0.125				
		CD103+PD1+	0.713	0.021	0.738	0.015				
		CD103+TIM3+	0.579	0.079	0.732	0.016				
		CD103+CTLA4+	0.774	0.009	0.738	0.015				
		CD103+LAG3+	0.669	0.049	0.686	0.041				
	CD8+ T	PD1+	0.353	0.316			0.226	0.531		
		TIM3+	0.549	0.100			0.561	0.092		
		CTLA4+	0.470	0.170			0.305	0.392		
		LAG3+	0.409	0.241			0.396	0.257		
		CD103+PD1+	0.354	0.316			0.372	0.290		
		CD103+TIM3+	0.573	0.083			0.537	0.110		
		CD103+CTLA4+	0.488	0.153			0.317	0.372		
		CD103+LAG3+	0.445	0.197			0.463	0.177		
	NK	PD1+	0.126	0.748					0.435	0.242
		TIM3+	0.677	0.032					0.762	0.010
		CTLA4+	0.232	0.519					0.427	0.219
		LAG3+	−0.018	0.969					0.541	0.210
		CD103+PD1+	0.072	0.878					0.270	0.558
		CD103+TIM3+	0.728	0.026					0.703	0.035
		CD103+CTLA4+	−0.025	0.949					0.536	0.137
		CD103+LAG3+	0.029	0.956					0.319	0.538

Immune check point marker expressing CD103$^+$, CD4$^+$ T cells strongly correlate with CTC number

To investigate the role of the tumor and immune cell biomarkers in predicting CTCs, the relationship between tumor and immune marker expression with CTCs was further investigated. We used Spearman rank correlation analysis to rank correlation between variables rather than the absolute values. The percentage of each of the cancer and immune marker expressing cells were compared against CTC numbers. The percentage was taken either as a fraction of the total TILs or the CD4$^+$, CD8$^+$ T cell, or NK cell populations. Dual marker expressing cell populations were also compared against CTCs [Fig. 4].

This statistical analysis revealed a strong correlation of CTC with TIM-3, PD-1, CTLA-4, and LAG-3 expressing lymphocytes, especially within the CD103$^+$, CD4$^+$ T cell phenotype [Table 2 and Fig. 4]. In particular, CD4+, CD103+ T-cells expressing PD-1, LAG3, and especially CTLA4 had strong, statistically significant correlations with the presence of CTCs. Correlations with CTCs were also observed with CD103 and HLA-DR double positive lymphocytes [Table 2].

To further characterize this cell type, we stained the same sample preparation with CD4, CD25, CD127, and CCR5 [Fig. 5]. All lung cancer samples with CTCs demonstrated that the CD4+, CD103+ cells expressed FoxP3 and these cells also expressed CCR5, a chemokine receptor involved in chemotaxis of immune cells in response to CCL5.

Discussion

Metastasis accounts for 90% of all cancer death. The complete mechanism causing metastasis is still largely unknown [21]. Due to the limitations of established technologies, investigations were either performed with IHC to study limited number cancer markers or immune markers, or with bulk lysed cancer tissue samples for RNA expression [22], and DNA content. High-parametric multiplexed biomarker expression investigation at the single cell level has proven to be difficult especially as it relates to utility in a clinical laboratory setting.

In this study, we dissociated NSCLC solid cancer tissues into single cells using previously published methods [12, 13] and following CAP approved guidelines [18]. The cells were stained with cancer and immune markers as well as a marker for cell cycle showing DNA content. High-parametric flow cytometry allowed us to study the contributions of cancer markers, immune markers and DNA content in cancer metastasis. Our study was designed to study both the cancer and the immune response in the tumor microenvironment [TME]. In parallel, peripheral blood samples from the same patients were also collected to isolate, enumerate and analyze the CTCs as potential surrogate indicator for cancer metastasis.

Consistent with the high level of PD-1 expression on lymphocytes in our cohort, our data showed increased aneuploid, PD-L1$^+$ cancer cells to be part of the predictive algorithm correlating with CTC and presumably cancer metastasis. In contrast, the cancer stem cells (CD44$^+$E-cad$^-$) significantly inversely correlated with CTCs suggesting the presence of a high number of quiescent cancer stem cells in the same tissue mass.

We also showed that DNA instability (as indicated by elevated DNA index) was a highly weighted parameter in our algorithm that significantly correlated with CTCs. This is consistent with a recent study on data collected from 5255 samples from 12 cancer types that revealed the correlation of aneuploidy and cancer “hallmarks”. The investigators demonstrated the correlation of aneuploidy with markers of cell proliferation, immune evasion and reduced response to immunotherapy [11]. Our results on the correlation of aneuploidy and immune suppression with cancer metastasis are consistent with this study.

We also addressed the role of tumor cell markers in predicting the presence of CTCs. EGFR was expressed in both diploid and aneuploid cells suggesting either genetic amplification of EGFR gene or other sig-

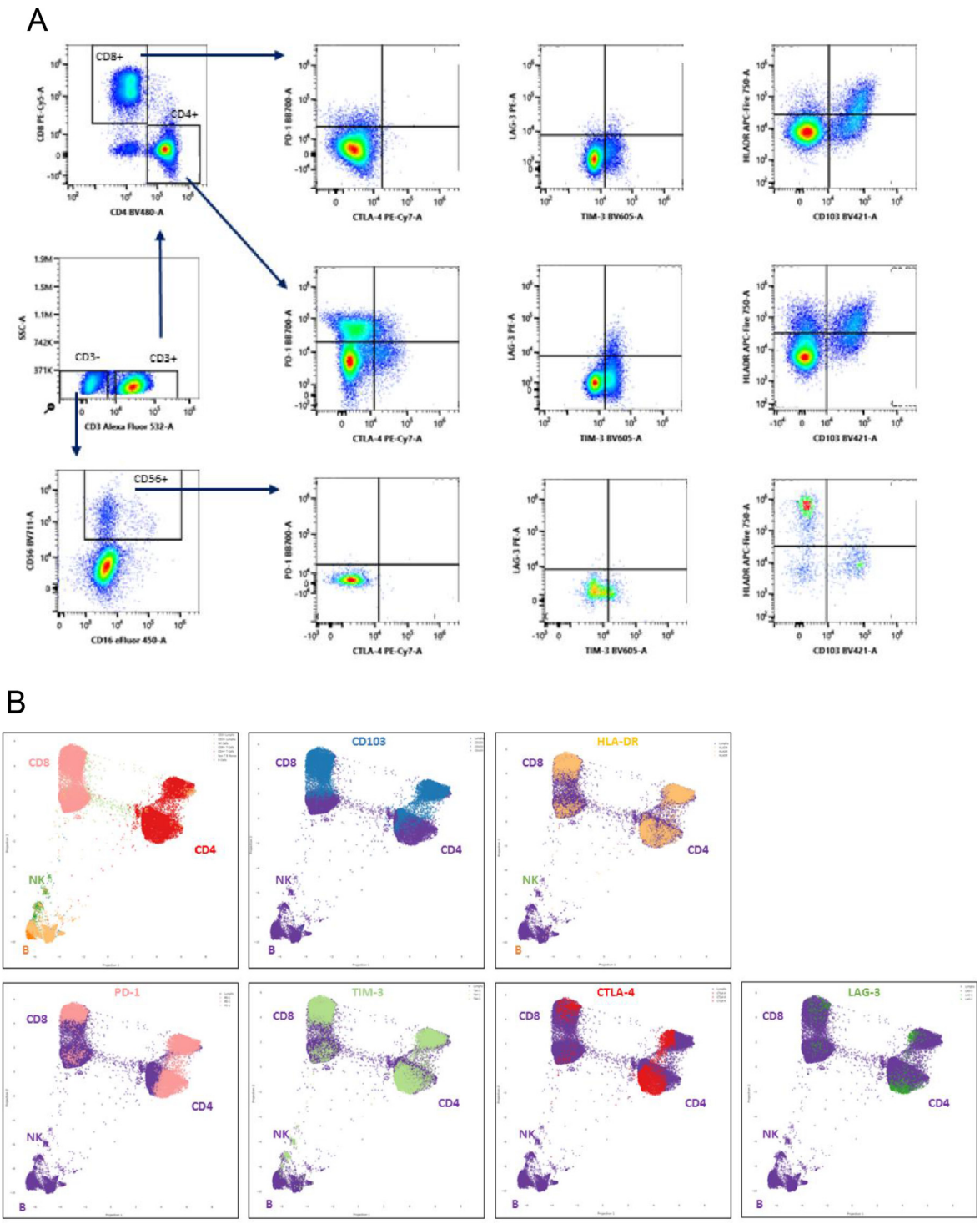

Fig. 3. Flow analysis of immune marker expressions.
(A). $CD45^+$ immune cells were gated into $CD4^+$, $CD8^+$ T cells and NK cells. The expression of immune checkpoint markers and CD103, HLA-DR were interrogated on each of these immune cell subsets.
(B). UMAP analysis. Tumor infiltrated lymphocytes [TILs] were separated into distinct $CD8^+$, $CD4^+$ T cells, B cells and NK cells. The cells expressing CD103, HLA-DR, PD-1, TIM-3, CTLA-4 and LAG-3 are shown in separate plots. Data presented is from Sample 1.

naling pathway activation might have contributed to the EGFR expression. The ALK expressing cells also expressed high level EGFR and possessed high DNA content suggesting there might be other genetic alteration occurring simultaneously with ALK fusion which was previously overlooked. Cleaved caspase 3 is in a common apoptotic pathway for both death receptors and mitochondrial cell death. The high level of lymphocytes going through apoptosis further demonstrated the immune suppressive mechanism utilized by cancer in these study patients.

The immune system, however, plays a dual role in cancer development. It suppresses cancer by destroying cancer cells or by inhibiting cancer growth, but ironically through its immune regulatory mechanisms [primarily Treg cells and myeloid suppressive cells], it can also

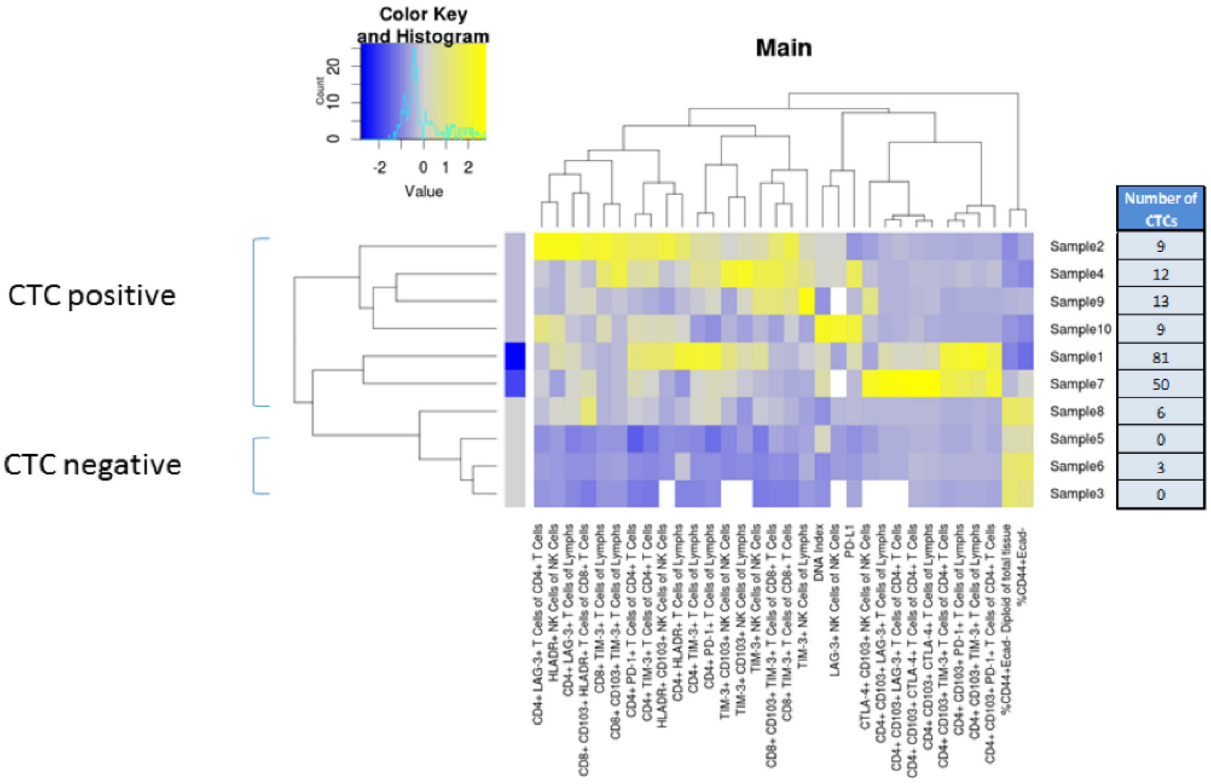

Fig. 4. Hierarchical clustering of various cell frequencies across all patient samples. Clustering analysis was performed using Euclidean distance on scaled data. Only data with Spearman R greater than 0.5 were included in the clustering. The cutoff for CTC positive and negative is 5 CTCs per 4 mL peripheral blood based on assay LOD.

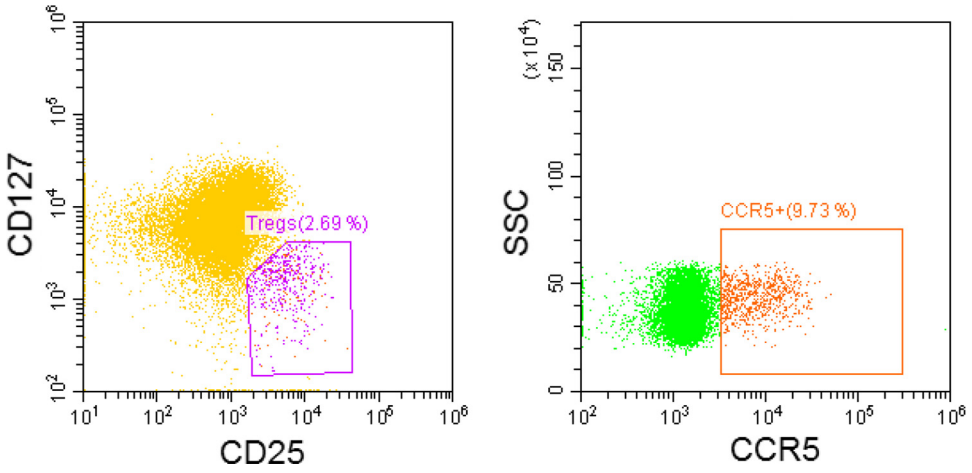

Fig. 5. Representative dot blot analysis of CCR5 expression on Treg (CD4, CD25+, CD127-) single cells from homogenized NSCLC tissue.

promote cancer growth by inhibiting cell-mediated immunity, effector T-cell proliferation, and by selecting for cancer cells that escape immune surveillance [23, 24]. Our results are consistent with this dynamic of the immune system in the cancer microenvironment.

Significantly, our results showed that immune checkpoint markers accounted for significant correlations to CTCs. These results directly correlated CTCs with known immune inhibitory function mediated by checkpoint markers expressed on immune cell subsets. Interestingly, the expression of these markers on $CD4^+$ cells, in contrast to commonly recognized $CD8^+$ cytotoxic T cells [25], had the stronger correlation. The association of PD-1 expression on $CD4^+$ T cells with clinical outcome has been reported albeit by only one other group [26] and this observation was in peripheral blood rather than the direct analysis of primary tumor as in the present study.

Specifically, we found the expression of the checkpoint markers on $CD103^+$, $CD4^+$ T cells correlated with CTCs. CD103 is the α_E unit of $\alpha_E\beta_7$ integrin expressing on tumor infiltrating immune cells [19, 20]. CD103 is expressed on tumor infiltrating regulatory T-cells (Treg) and some have suggested that $CD103^+$ Treg are more potent inhibitors of T cell proliferation than conventional Treg [27]. In addition to CD103, CTLA-4 expressing T-regs in our corhort correlated with CTCs. Anti-CTLA therapy with ipilimumab [Yervoy], in the treatment of melanoma patients significantly reduced FOXP3+ Treg cells in the tumor tissues particularly in clinical responders [28, 29]. Other studies showed that FOXP3+ T-reg cells were depleted in tumor tissues by anti-CTLA-4 thereby augmenting tumor specific immunity [30, 31].

Similarly, studies of the C-X-C chemokine CXCR2 in pancreatic cancer demonstrated an immunosuppressive effect [32]. The proposed

mechanism of action of CXCR-2 is to act as a homing beacon for immune cells, specifically to attract neutrophils and myeloid suppressor cells [32]. In tumors, CXCR-2 is overexpressed on immune cells found in the tumor microenvironment of pancreatic cancer. Similarly, therapeutics targeting CCR5 have been shown to have anti-tumor and anti-metastatic activity [33]. CCR5 inhibitors such as Maraviroc [Pfizer, Inc], Leronlimab [Cytodyn, Inc], and newer compounds such as OB-002 [Orion Biotechnologies, Inc] are newer additions to the immune-oncology armamentarium. In addition to potentially inhibiting the influx of Treg cells into the tumor, CCR5 inhibitors also have been shown to cause repolarization of macrophages to an anti-tumor phenotype in colorectal cancer [33].

The unsupervised Spearman clustering analysis in the present study clearly separated the patients with positive CTCs from negative CTCs. These data illustrate the strength of single cell analysis in sorting through heterogeneous marker expression on tumor cells that would be lost using technologies that extract nucleic acids from the specimen without the cellular context. Further, the data generated from multiparametric flow data identified a signature that predicts CTCs, and potentially cancer metastasis, which may provide predictive, actionable information to patient management and new therapies.

Conclusions

In summary, a biomarker or set of biomarkers, as we have identified in this pilot study that identifies drug targets on cells within the tumor microenvironment that have inhibitory effects on the anti-tumor immune response like T-regs is critically important to devise multi-drug treatment strategies that will potentially provide long-lasting response in a higher percentage of patients. These data await large scale, placebo controlled trials to confirm clinical relevance.

Declaration of Competing Interest

Xiaoyang Wang, Pin-I Chen, Keith Shults, and Bruce K Patterson are full time employees of IncellDx Inc.

Maria Jaimes and Huimin Gu are full time employees of Cytek Biosciences Inc.

Santosh Putta is full time employee of Qognit Inc.

Vishal Sharma, Will Chow, Priya Gogoi, and Kalyan Handique are full time employees of Celsee Inc.

CRediT authorship contribution statement

Xiaoyang Wang: Writing - original draft, Supervision. **Maria Jaimes:** Investigation. **Huimin Gu:** Investigation. **Keith Shults:** Investigation, Formal analysis. **Santosh Putta:** Formal analysis. **Vishal Sharma:** Investigation. **Will Chow:** Investigation. **Priya Gogoi:** Project administration. **Kalyan Handique:** Supervision. **Bruce K Patterson:** Writing - original draft, Supervision.

Ethical approval statement

Fresh tissues were obtained from 12 NSCLC cases by Spectrum Health (Grand Rapids, Michigan) following informed consent. Date of collection, age, sex, ethnicity,diagnosis, primary tumor size, and American Joint Committee on Cancer (AJCC) classification were recorded.

Funding sources

This research did not receive any specific grant from funding agencies in the public, commercial, or not-for-profit sectors.

Supplementary materials

Supplementary material associated with this article can be found, in the online version, at doi:10.1016/j.tranon.2020.100953.

References

[1] D.H. Johnson, J.H. Schiller, P.A. Bunn, Recent clinical advances in lung cancer management, J. Clin. Oncol. 32 (2014) 973–982.
[2] A.G. Pallis, A review of treatment in non-small-cell lung cancer, Eur. Oncol. Haematol. 8 (2012) 208–212.
[3] M Sambi, L Bagheri, M.R. Szewczuk, Current challenges in cancer immunotherapy: multimodal approaches to improve efficacy and patient response rates, J Oncol (2019) PMID:30941175 .
[4] M Tamminga, et al., Circulating tumor cells in advanced non-small cell lung cancer patients are associated with worse tumor response to checkpoint inhibitors, J. Immunol. Ther. Cancer 7 (173) (2019) 1–9.
[5] R.S. Heist, PD-(L)1 inhibitors and CTLA-4 inhibitors: rationale for combinations and recent data in non-small cell lung cancer, Am. J. Hematol. Oncol. 11 (2015) 21–25.
[6] A.C. Anderson, N. Joller, V.K. Kuchroo, Lag-3, tim-3, and TIGIT: coinhibitory receptors with specialized functions in immune regulation, Immunity 44 (2016) 989–1004.
[7] A.C. Anderson, Tim-3: an emerging target in the cancer immunotherapy landscape, Cancer Immunol. Res. 2 (2014) 393–398.
[8] D.S. Micalizzi, D.A.; Haber, S. Maheswaran, Cancer metastasis through the prism of epithelial-to-mesenchymal transition in circulating tumor cells, Mol. Oncol. 11 (2017) 770–780.
[9] J Kapeleris, et al., The prognostic role of circulating tumor cells (CTCs) in lung cancer, Front. Oncol. (2018), doi:10.3389/fonc.2018.00311.
[10] H.E. Danielsen, M. Pradhan, M. Novelli, Revisiting tumour aneuploidy-the place of ploidy assessment in the molecular era, Nat. Rev. Clin. Oncol. 13 (2016) 291–304.
[11] T. Davoli, H. Uno, E.C. Wooten, S.J. Elledge, Tumor aneuploidy correlates with markers of immune evasion and with reduced response to immunotherapy, Science 355 (2017) 6322–6355.
[12] A. Chargin, Quantification of PD-L1 and PD-1 expression on tumor and immune cells in non-small cell lung cancer [NSCLC] using non-enzymatic tissue dissociation and flow cytometry, Cancer Immunol. Immunother. 65 (2016) 1317–1323.
[13] S. Young, Concordance of PD-L1 Expression Detection in Non–Small Cell Lung Cancer [NSCLC] Tissue Biopsy Specimens Between OncoTect iO Lung Assay and Immunohistochemistry [IHC], Am. J. Clin. Pathol. 150 (2018) 346–352.
[14] Y-L. Chen, et al., Novel circulating tumor cell-based blood test for the assessment of PD-L1 protein expression in treatment-naive, newly diagnosed patients with non-small cell lung cancer, Cancer Immunol. Immunother. 68 (2019) 1087–1094.
[15] P. Gogoi, Development of an automated and sensitive microfluidic device for capturing and characterizing circulating tumor cells [CTCs] from clinical blood samples, PLoS One 11 (2016), doi:10.1371/journal.pone.0147400.
[16] McInnes, L.; and Healy, J. UMAP: uniform manifold approximation and projection for dimension reduction. 2018 arXiv:1802.03426v1
[17] L.J.P. Van Der Maaten, G.E. Hinton, Visualizing high-dimensional data using t-sne, J. Mach. Learn. Res. 9 (2008) 2579–2605.
[18] Current CAP Protocols 2013. Hematologic v3.1.0.1.
[19] J.R. Webb, K. Milne, B.H. Nelson, Location, location, location: CD103 demarcates intraepithelial, prognostically favorable CD8[+] tumor-infiltrating lymphocytes in ovarian cancer, Oncoimmunology 3 (2014), doi:10.4161/onci.27668.
[20] F.L. Komdeur, et al., CD103+ tumor-infiltrating lymphocytes are tumor-reactive intraepithelial CD8+ T cells associated with prognostic benefit and therapy response in cervical cancer, Oncoimmunology 6 (2017), doi:10.1080/2162402X.2017.1338230.
[21] T.N. Seyfriend, L.C. Huysentruyt, On the origin of cancer metastasis, Crit Rev Oncol 18 (2013) 43–73.
[22] P.L. Chen, et al., Analysis of immune signatures in longitudinal tumor samples yields insight into biomarkers of response and mechanisms of resistance to immune checkpoint blockade, Cancer Discov. 6 (2016) 827–837.
[23] R.D. Schreiber, L.J. Old, M.J. Smyth, Cancer immunoediting: integrating immunity's roles in cancer suppression and promotion, Science 331 (2011) 1565–1570.
[24] D. Mittal, M.M. Gubin, R.D. Schreiber, M.J. Smyth, New insights into cancer immunoediting and its three component phases-elimination, equilibrium and escape, Curr. Opin. Immunol. 27 (2014) 16–25.
[25] J.S. Yi, M.A.; Cox, A.J. Zajac, T-cell exhaustion: Characteristics, causes and conversion, Immunology 129 (2010) 478–481.
[26] H. Zheng, et al., Expression of PD-1 on CD4+ T cells in peripheral blood associates with poor clinical outcome in non-small cell lung cancer, Oncotarget 7 (2016) 56233–56240.
[27] D. Anz, et al., CD103 is a hallmark of tumor-infiltrating regulatory T cells, Int. J. Cancer 129 (2011) 2417–2426.
[28] A. Verma, et al., T-Regulatory cells in tumor progression and therapy, Cancer Manag. Res. 11 (2019) 10731–10747.
[29] D. Ha, et al., Differential control of human Treg and effector T cells in tumor immunity by Fc-engineered anti–CTLA-4 antibody, PNAS 116 (2019) 609–618.
[30] T.R. Simpson, et al., Fc-dependent depletion of tumor-infiltrating regulatory T cells co-defines the efficacy of anti-CTLA-4 therapy against melanoma, J. Exp. Med. 210 (2013) 1695–1710.
[31] M.J. Selby, et al., Anti-CTLA-4 antibodies of IgG2a isotype enhance antitumor activity through reduction of intratumoral regulatory T cells, Cancer Immunol. Res. 1 (2013) 32–42.
[32] C.W. Steele, et al., CXCR2 inhibition profoundly suppresses metastases and augments immunotherapy in pancreatic ductal adenocarcinoma, Cancer Cell 29 (2016) 832–845.
[33] N. Halama, Tumoral immune cell exploitation in colorectal cancer metastases can be targeted effectively by anti-CCR5 therapy in cancer patients, Cancer Cell 29 (2016) 587–601.